PERIODICO di MINERALOGIA
established in 1930

DIPARTIMENTO
DI SCIENZE DELLA TERRA
SAPIENZA
UNIVERSITÀ DI ROMA

An International Journal of
Mineralogy, Crystallography, Geochemistry,
Ore Deposits, Petrology, Volcanology
and applied topics on Environment, Archaeometry and Cultural Heritage

Prediction of economic potential of deep blind mineralization by Fourier transform of a geochemical dataset

Hossein Mahdiyanfar *

Department of Mining Engineering, University of Gonabad, 9691957678 Gonabad, Iran

ARTICLE INFO

Submitted: July 2019
Accepted: October 2020
Available on line: December 2020

* Corresponding author:
Hssn.shahi@gmail.com

DOI:10.13133/2239-1002/16739

How to cite this article:
Mahdiyanfar H. (2021)
Period. Mineral. 90, 123-136

ABSTRACT

The identification of blind and disseminated mineral deposits is an important challenge in mining exploration. This research presents a quantitative approach to predict a deep, hidden disseminated mineralization using a novel approach named Frequency Coefficient Method (FCM) in mining geochemistry. In deep mineral deposits, the processes of ore formation produce geochemical anomalies at the surface, which have distinct wavelengths and frequencies. These deposits can be detected using geochemical signals by processing Fourier transform and interpreting these frequency signals. In particular, analyses of a certain geochemical dataset in the frequency domain (FD) prove to be an effective tool for identifying deep ore-formation processes and hence, they can potentially discover hidden mineralization at depth before borehole drilling is carried out. In this study, FCM was applied to a geochemical dataset made of 104 soil and whole rock elemental analyses from the Au-bearing vein system of Tanurcheh (Khaf-Daruneh belt, north-east Iran) to predict the uneconomic nature of that Au mineralization at depth. Such conclusion was tested and validated by the Au grade distribution of six exploration boreholes.

Keywords: gold mineralization; frequency anomaly; Fourier transform; dispersed mineralization zone; pattern recognition.

INTRODUCTION

The discrimination between blind and dispersed mineralization zones at depth using geochemical data is one of important aims in mining exploration. This issue has been surveyed in the spatial domain based on alteration (Hannington et al., 2003) and mineral deposit type and enrichment and depletion of geochemical haloes (Carranza and Sadeghi, 2012).

Zonality method, based on the geochemical distribution of elements, was applied for distinguishing of blind mineralization and dispersed mineralization area in certain ore deposits (Grigorian, 1985, 1992; Beus and Grigorian, 1977; Distler et al., 2004; Gundobin, 1984; Ziaii et al., 2011). Furthermore, other approaches have scarcely been performed for identifying hidden mineralization zones based on the erosion horizons of geochemical data in the spatial domain (Levinson, 1980; Grigorian, 1992; Ziaii et al., 2007, 2011; Ziaii et al., 2012).

The identification of deep mineralization or non-mineralization zones as a challenging problem can also be performed using Fourier transform and frequency domain (FD) of surface geochemical data (Mahdiyanfar, 2019). In addition to the spatial domain, the geochemical data can be interpreted in FD. The analysis of geochemical data in FD may be providing important information about the mineralization process that may not be achieved in the spatial domain. The variety of geological and mineralization processes can create different geochemical frequency signals at the surface. Hence, these complicated processes can be discriminated using the interpretation

of geochemical signals in FD (Shahi et al., 2014, 2015, 2016). Fourier transform as a data mining method has widely been used for many engineering and mathematical topics (Osgood, 2019). Several researchers utilized the Fourier transform for interpreting geochemical data in FD. The fractal method has been applied for separation of geochemical anomaly and background in the FD (Wang and Zuo, 2015a; Cao and Cheng, 2012; Cheng and Zhao, 2011; Zuo, 2011 a,b; Hassani et al., 2009; Cheng et al., 2000; Cheng, 1999; Zuo et al., 2012, 2013). Parsa et al. (2017) applied the S–A fractal method to multifractal gridded data and delineated the multi-element geochemical anomalies at the Ahar Cu mineralization. Ghezelbash et al. (2019a) identified a mineralization factor consisting of Cu-Au-Mo-Bi elements using two-stage factor analysis and this multi-element factor was interpreted by using the S-A fractal method and then, the geochemical anomaly was delineated in the Varzaghan porphyry Cu mineralization area. Shokouh Saljoughi et al. (2018) compared the S-A fractal model to the concentration - area fractal and the U-statistic method and obtained geochemical anomalies in the Avanj porphyry system in FD. Ghezelbash et al. (2019b) performed the S–A fractal method on the geochemical data set obtained by multifractal Kriging interpolation technique and identified the geochemical anomaly.

Zuo and Wang (2015) described the application of fractal method in the FD. They mentioned the disadvantage of S-A fractal method in the exploration of hidden ore deposits. Wang and Zuo (2015b) presented a Matlab-based program for geochemical data processing using the fractal method in the FD.

Shahi et al. (2014) showed that there is a relationship between the wavelength values of geochemical data and the depth of mineral deposits. Shahi et al. (2014, 2015, 2016) indicated that very low frequency geochemical signals are mostly related to background values and deep mineral deposits. Shahi et al. (2016) demonstrated that mineralization processes produce different wavelengths and frequencies of geochemical data at the surface and successfully applied the FCM idea for identifying deep blind copper porphyry deposits. In this research, as a state of the art for the application of FCM, the strong surface Au geochemical anomaly in the Tanurcheh area was successfully evaluated as a deep dispersed mineralization zone.

STUDIED AREA

The Tanurcheh area is located in the eastern edge of the 1:100,000 scale geological map of Feyzabad (NE Iran) on the Khaf-Daruneh geological belt. The geological map of the Tanurcheh area is shown in Figure 1. This map was drawn by using 116 samples from lithological units and alteration areas and the respective thin sections in the 1:5,000 scale. Tanurcheh area has a specific tectonic situation and a large variety of lithological units and intrusive bodies.

Three major lithological units consisting of pyroclastics and lavas and intrusive igneous rocks that are related to the Tertiary age can be distinguished in this area. The pyroclastic rocks mainly consist of tuff, lapilli-tuff and crystal-tuff. The lavas included rhyolite, dacite, rhyodacite and latite rocks, which are widely distributed over the surface and are older than the intrusive rocks. Rhyolites have a grey and purplish appearance and the alteration products are mostly silicified, sometimes sericitized and seldom chloritized. Dacites and rhyodacites have porphyritic texture whose alteration products are silicified and, limitedly, sericitized. Latites have porphyritic texture and their major alteration is silicification. The alteration map of study area in the scale of 1:5,000 is shown in Figure 2.

Distinct intrusive magmatic activities were identified in this area. The intrusive igneous rocks consist of plutonic and semi-plutonic igneous rocks and can be classified into three groups: porphyry-monzonite, quartz-monzonite and porphyry-diorite. The stock quartz-porphyry mass as an important intrusive rock is a priority for prospecting of gold mineralization.

Secondary iron oxides are usually in veins and veinlets and brecciated or disseminated zones. Veinlets of stock-work, semi-parallel veinlets with secondary iron oxides, are located in the phyllic alteration zone. Secondary iron oxides such as hematite, goethite and limonite are distributed over the altered area of Tanurcheh that can be the result of oxidization of sulfide minerals. In addition to silicification in different parts of the Tanurcheh area, a complex of silica veins and veinlets enriched by secondary iron oxides also developed. Mineralization within silica is in the form of vuggy quartz type with fine pyrite crystals disseminated in the rock texture. Pyrite in later phases appear with veins, veinlets and breccias and is associated with secondary iron oxides, mainly in the form of goethite (Karimpour, 2004).

MATERIALS AND ANALYTICAL METHODS

Geochemical sampling and analytical method

Rock samples were collected from the alteration system of Tanurcheh (around 350 ha). 104 lithogeochemical samples were collected in different survey in order to study the assay of gold, copper and other elements. These samples were analyzed for 24 elements (Au, Al, As, Ba, Ca, Co, Cr, Cu, Fe, K, La, Mg, Mn, Mo, Na, Ni, P, Pb, S, Sc, Sr, Ti, V, Zn) using ICP-AES at OMAC (Ireland) and ALS CHEMEX (Canada). The location of these samples is shown in Figure 3. These data are not presented since they

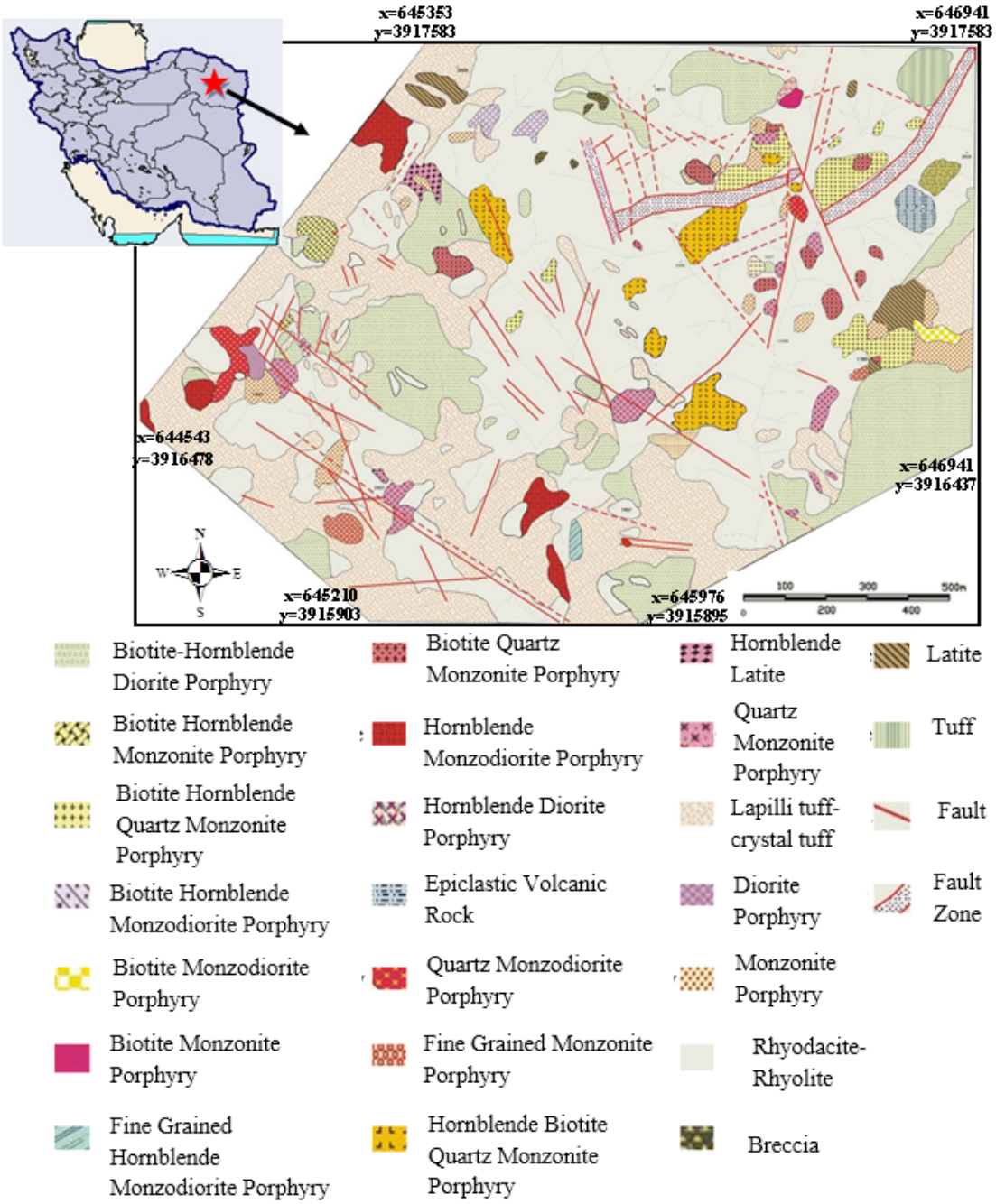

Figure 1. Geological map of Tanurcheh mineralization area in the 1:5,000 scale.

covered by a confidentiality agreement. They were taken by Zarmehr gold company (ZGC) and Riotinto company from alteration zones, outcrops of sulfide mineralization, especially pyrite and in some cases chalcopyrite, secondary iron oxides, silica ± iron oxides veinlets and box-works of iron oxides and areas with hydrothermal or faulted breccia (Karimpour, 2004).

Fourier transform decomposes a function or signal into various components based on frequency content (Hassani et al., 2009). The geochemical map can be considered as a two-dimensional signal in the spatial domain. Fourier transform can decompose the two-dimensional signals, e.g. geochemical map to different sinusoidal wavelengths. The geochemical distribution maps that are obtained by interpolating the geochemical data contain different frequency signals (Cheng et al., 2000). Hence, the surface

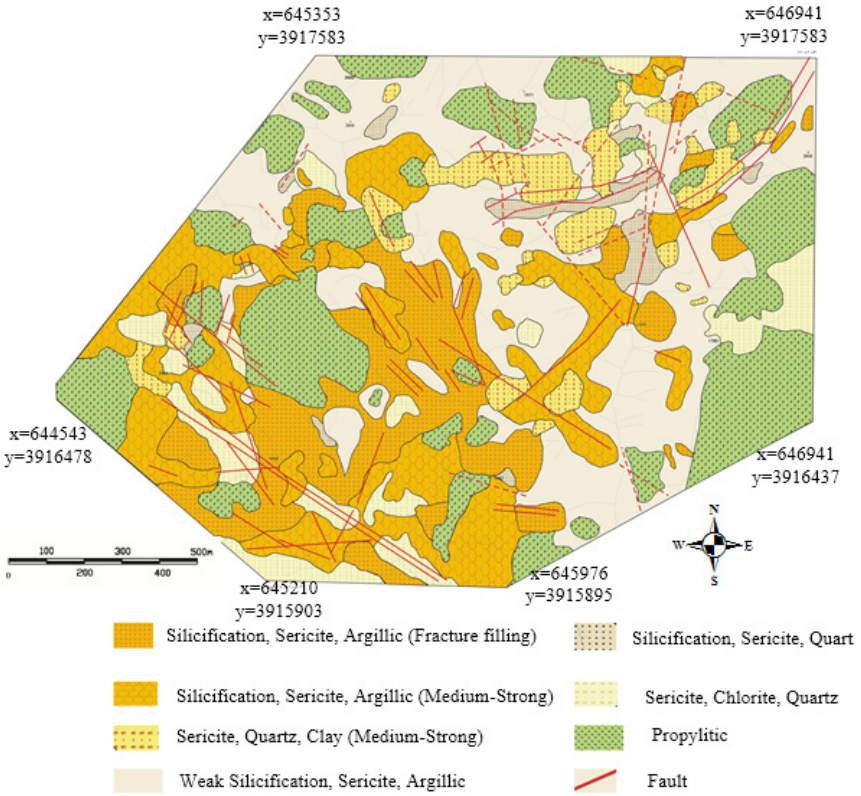

Figure 2. Alteration map of Tanurcheh mineralization area in the 1:5,000 scale.

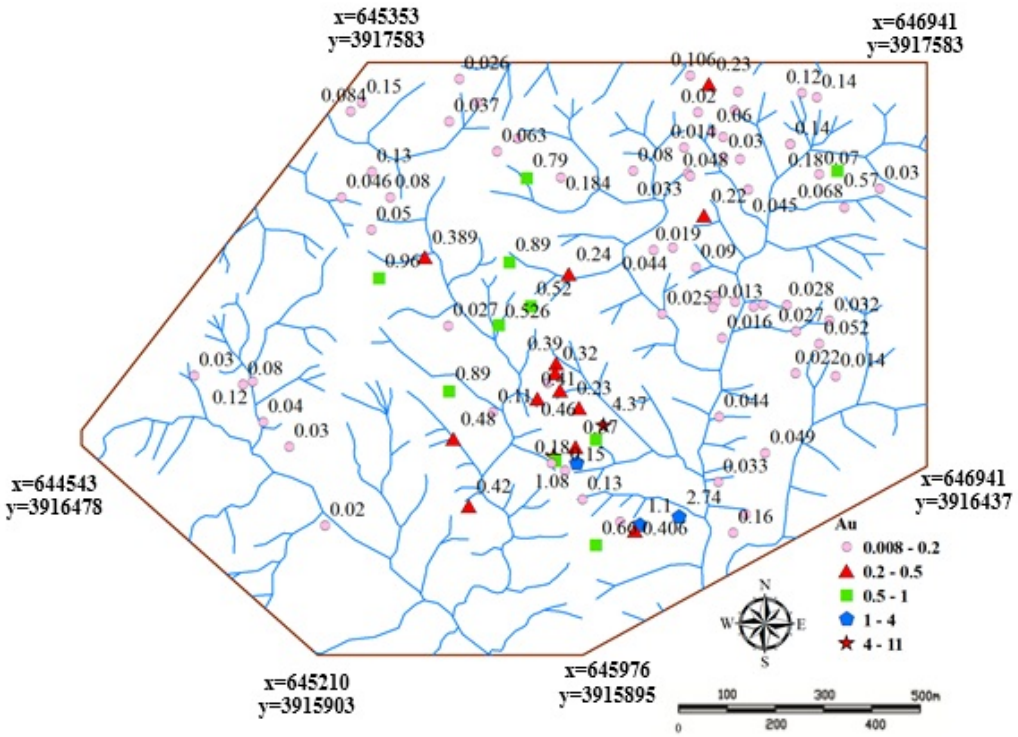

Figure 3. The locations of surface geochemical samples that were taken from alteration zones and outcrops of mineralization in Tanurcheh area.

geochemical data, concentrations of elements at the surface, can be transformed to FD using two-dimensional Fourier transform (e.g. Shahi et al., 2016; Zuo, 2011 a,b; Zuo and Wang, 2015).

Cheng (2012) demonstrated that the concentration of mineralization elements at the surface is depending at which depth the ore deposits is located. He showed that the outcropping and shallow ore deposits produce high concentrations at the surface while mineralization at about 1 km below the surface has small concentrations at the surface. These low concentrations show low variabilities (low frequency signals) at the surface while the surface mineralization with strong outcropped veins are generally associated with high variabilities (Cheng, 2014; Shahi, 2017). The concept of frequency of geochemical data is related to the degree of variability of the elements. Therefore, mineral deposits at different depths produce different frequency geochemical signals at the surface (Shahi et al., 2015, 2016).

Zuo and Wang (2015) presented a simulated geochemical pattern hosting ore deposits at different burial depths. They demonstrated the deeper the ore deposit the weaker the concentration distribution at the surface and the distribution map had low frequency signal that were almost not distinguishable from the background. Shahi et al. (2016) introduced FCM as an effective technique in FD of geochemical data. FCM showed a significant relationship between the mineralization depth and the frequencies of surface geochemical signals (Shahi et al., 2016). The mineralization intensity and the importance of mineralization elements in various frequency bands (FBs) can be determined based on this approach. There are four-steps for FCM application, as follows:

Step 1: Two-dimensional Fourier transform:

The surface geochemical distribution map as a spatial signal is transformed to FD using two-dimensional Fourier transform. Eq. 1 is applied for this transformation (Dobrin and Savit, 1988):

$$F(K_x,K_y)=\int_{-\infty}^{\infty}\int_{-\infty}^{\infty} f(x,y)\cos(K_x x+ K_y y)dxdy-\int_{-\infty}^{\infty}\int_{-\infty}^{\infty} f(x,y)\sin(K_x x+ K_y y)dxdy \quad (1)$$

where f(x, y) is geochemical map; Kx and Ky are "wave numbers" to EW and NS directions.

Finally, the geochemical map is converted to power spectrum distribution map that consists of power spectrum values and wave numbers in directions of the east-west and the north-south in the FD.

Step 2: Designation and implementation of filter functions:

Several filter functions are designed based on wave numbers and their power spectrum values. These filters are performed on the power spectrum maps for all elements and subsequently several FBs can be obtained.

Step 3: Extraction of mineralization component using Principal Component Analysis (PCA) method:

PCA is a multivariate statistical method to determine the relationship among the elements on the basis of correlation coefficients or covariance. PCA reduces the dimension of data and produces new independent variables named principal components. In this step, PCA method is performed on obtained FBs, to separately investigate the behavior of mineralization elements in the FD.

Step 4: Delineation of frequency coefficients diagram:

The frequency coefficients of mineralization elements are obtained from the mineralization factor in the PCA rotated component matrix. The FCM diagram is delineated by the frequency coefficients of elements versus the wave numbers of FBs. This diagram can determine frequency anomalies and mineralization zones at depth. The deep dispersed mineralized and non-mineralized zones cannot intensify the role of mineralizing elements in low FBs while the blind mineral deposits can effectively intensify the frequency coefficients of mineralization elements in mineralization factor in low FBs. The coefficients of mineralization elements in rotated component matrix obtained by PCA are detected as frequency coefficients of mineralization elements. On the other hand, the deep ore deposits produce low concentrations at the surface and their surface geochemical anomaly maps contain low frequency geochemical signals and form the frequency anomaly for low FBs. FCM diagram does not show any frequency anomaly for the deep dispersed mineralization zone for low FBs.

RESULTS AND DISCUSSION

Based on scattered sampling, some gold anomalies were observed. The descriptive statistics of Au in these surface samples are listed in Table 1. At the surface, silica veins are oxidized and sulfide minerals are strongly

Table 1. Descriptive statistics of original geochemical data.

	Minimum	Maximum	Mean	Std. Deviation	Variance	Skewness	Kurtosis
Au(ppm)	0.01	11.48	0.38	1.23	1.51	7.76	67.17

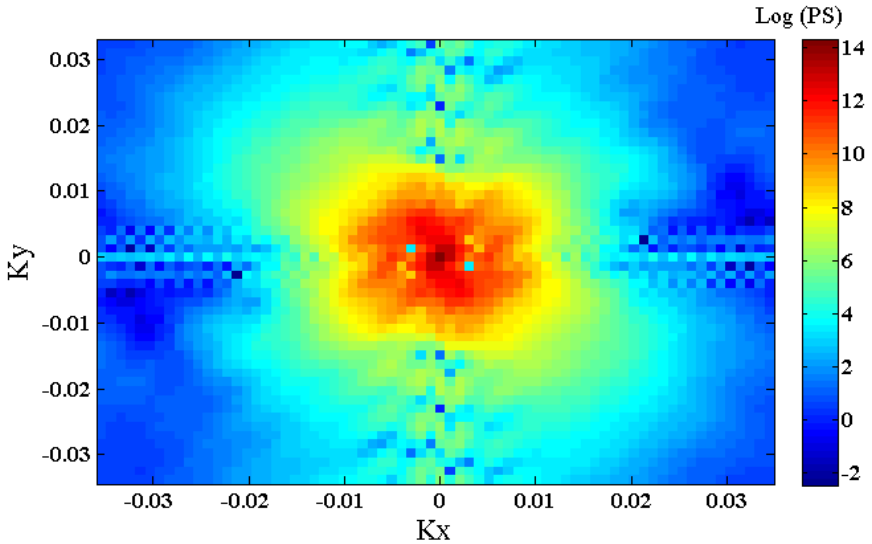

Figure 4. The power spectrum distribution map of Au in the FD that indicates the power spectrum values of different wavelengths in the directions of X and Y.

altered. This process has caused strong acid leaching of intrusive dioritic rocks around the veins. The geochemical anomalies based on soil and rock samples show very good coordination with mineralization in this area.

The original spatial distribution maps of elements were converted to FD by Fourier transform, individually and two components, including power spectrum and phases, were obtained for any of elements. The power spectrum distribution map for Au element is depicted in Figure 4. The power spectrum maps can provide a large amount of significant exploratory information about the mineral deposit.

The applied FCM scenario in this study is schematically illustrated in Figure 5. Eight filters were designed and applied on the power spectrum distribution maps for all of elements, individually (Table 2). G (K_x, K_y) as filter function is multiplied to the obtained power spectrum maps. These filters consist of low, band and high pass filters and are performed by decomposing the geochemical frequency signals. These filters remove some frequencies based their wave numbers from power spectrum map and various frequency bands (FBs) are obtained. The schematic maps of the filter functions and the obtained FBs are presented in Figure 6 and Figure 7, respectively.

In order to distinguish the behavior of gold mineralization in this area, PCA method was separately performed on these FBs and the mineralization factors were considered. The results of rotated component matrix for FB2, 7 and 8 are shown in Table 3. The results of other FBs are similar to these FBs while the variance values of principal components (PCs) obtained from PCA for FB2 (7 and 8) are reported in Table 4.

PCA has allowed to classify all 24 elements into 2 PCs in FB2 (Table 3). PCA, as a dimension reduction method, has properly separated the mineralization factor from the background component in the FD. PCs, 1 and 2, are related to the geochemical background and the mineralization process, respectively. PC2 as mineralization factor consists of Au, Ba, Cu, Co, P and S. Gold score in the geochemical background component is higher than the mineralization component. This fact shows that the behavior of Au is similar to the background elements such as Al, Ca and Na and the Au mineralization process does not hold the important role in this FB and these geochemical signals are more related to the background. PCA could divide all 24 elements in two PCs in FB7 and 8 (Table 3). PC1 and PC2 were recognized as background and mineralization components, respectively. Barium, Cu, Co and P are effective in PC2 as mineralization component. Gold does not have any significant role in the mineralization process while it is apparently related to the background PC. In these FBs, Au frequency signals are not related to the mineralization phase and are considered as background. The role of Au intensified in the background component and reduced in the mineralization process from the high to the low frequency signals (FB1 to FB8). Table 3 shows that Au has a key role in the first PC (background), especially for low FBs. In these cases, low frequency signals of mineralizing elements have strong role in the mineralization process. These frequency signals can be detected properly using PCA and the mineralizing elements will have important role in mineralization PC. The low frequency signals of mineralization elements in deep dispersed mineralization zones are more related

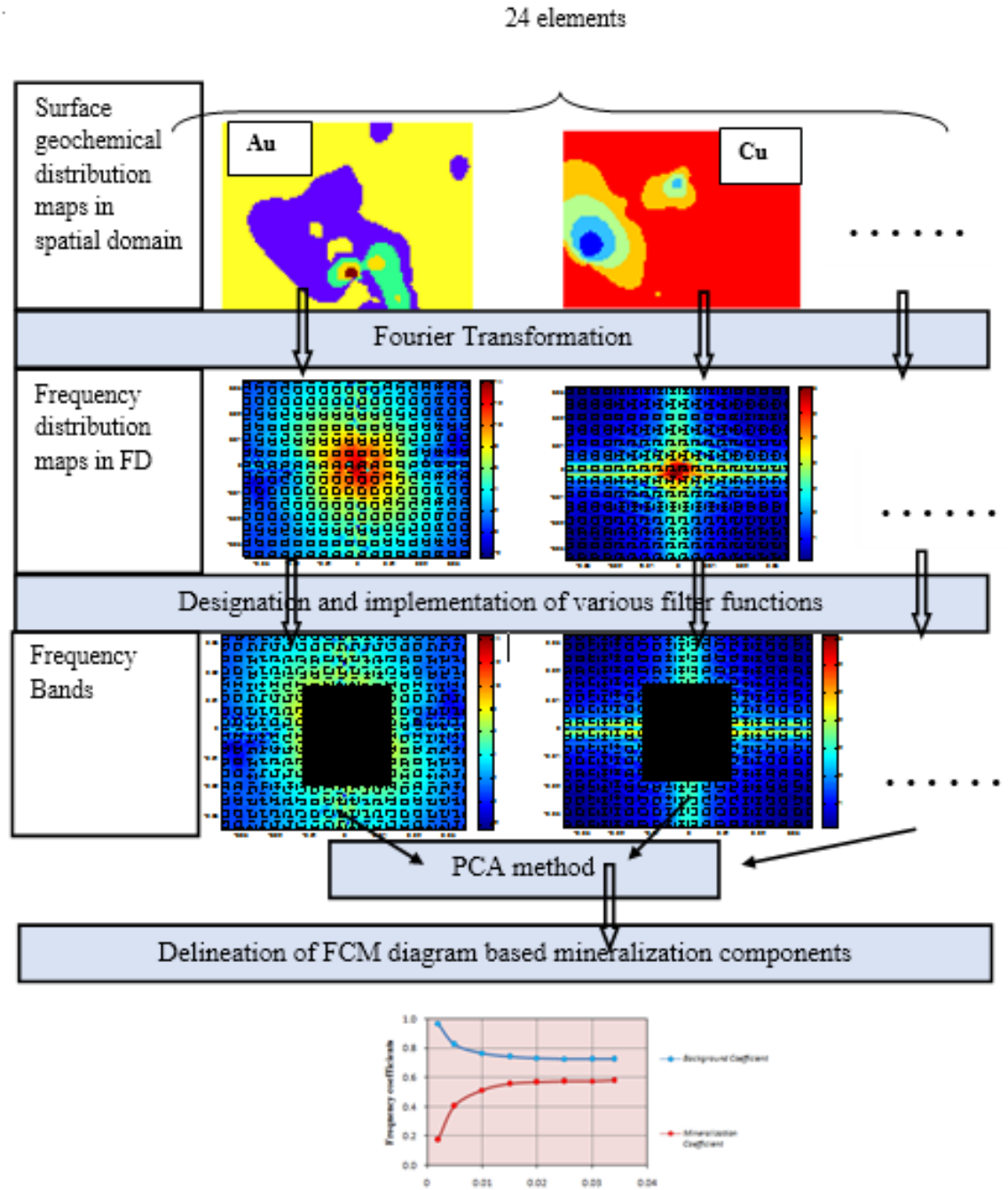

Figure 5. The schematic various steps for FCM in order to determining the behavior of mineralization elements in the FD.

to the background component. The obtained results of PCA on various FBs indicate there is a deep dispersed Au mineralization zone in the studied area.

The FCM diagram shows the importance of Au in the background and mineralization components in different FBs (Figure 8). In this diagram, the mineralization curve has a decreasing trend from the high to the low frequency signals while the trend of background curve increases toward the low frequencies. In FCM diagram, the high frequency coefficients values of Au in background curve indicate the Au mineralization process is not notable. There is a strong frequency background and very low frequency anomaly in the low FBs in this diagram. Shahi et al. (2014, 2016) demonstrated there is a relationship between the depth of mineralization zone and the frequency anomalies in the FD. The effects of

Table 2. The designed filter function based on the wave number values in the FD.

FB	Filter Function	FB	Filter Function
FB1	$G(k_x,k_y)=\begin{cases}1 & \lvert k_x\rvert \text{ and } \lvert k_y\rvert \le 0.034\\ o & \text{otherwise}\end{cases}$	FB5	$G(k_x,k_y)=\begin{cases}1 & \lvert k_x\rvert \text{ and } \lvert k_y\rvert \le 0.015\\ o & \text{otherwise}\end{cases}$
FB2	$G(k_x,k_y)=\begin{cases}1 & \lvert k_x\rvert \text{ and } \lvert k_y\rvert \le 0.03\\ o & \text{otherwise}\end{cases}$	FB6	$G(k_x,k_y)=\begin{cases}1 & \lvert k_x\rvert \text{ and } \lvert k_y\rvert \le 0.01\\ o & \text{otherwise}\end{cases}$
FB3	$G(k_x,k_y)=\begin{cases}1 & \lvert k_x\rvert \text{ and } \lvert k_y\rvert \le 0.025\\ o & \text{otherwise}\end{cases}$	FB7	$G(k_x,k_y)=\begin{cases}1 & \lvert k_x\rvert \text{ and } \lvert k_y\rvert \le 0.005\\ o & \text{otherwise}\end{cases}$
FB4	$G(k_x,k_y)=\begin{cases}1 & \lvert k_x\rvert \text{ and } \lvert k_y\rvert \le 0.02\\ o & \text{otherwise}\end{cases}$	FB8	$G(k_x,k_y)=\begin{cases}1 & \lvert k_x\rvert \text{ and } \lvert k_y\rvert \le 0.002\\ o & \text{otherwise}\end{cases}$

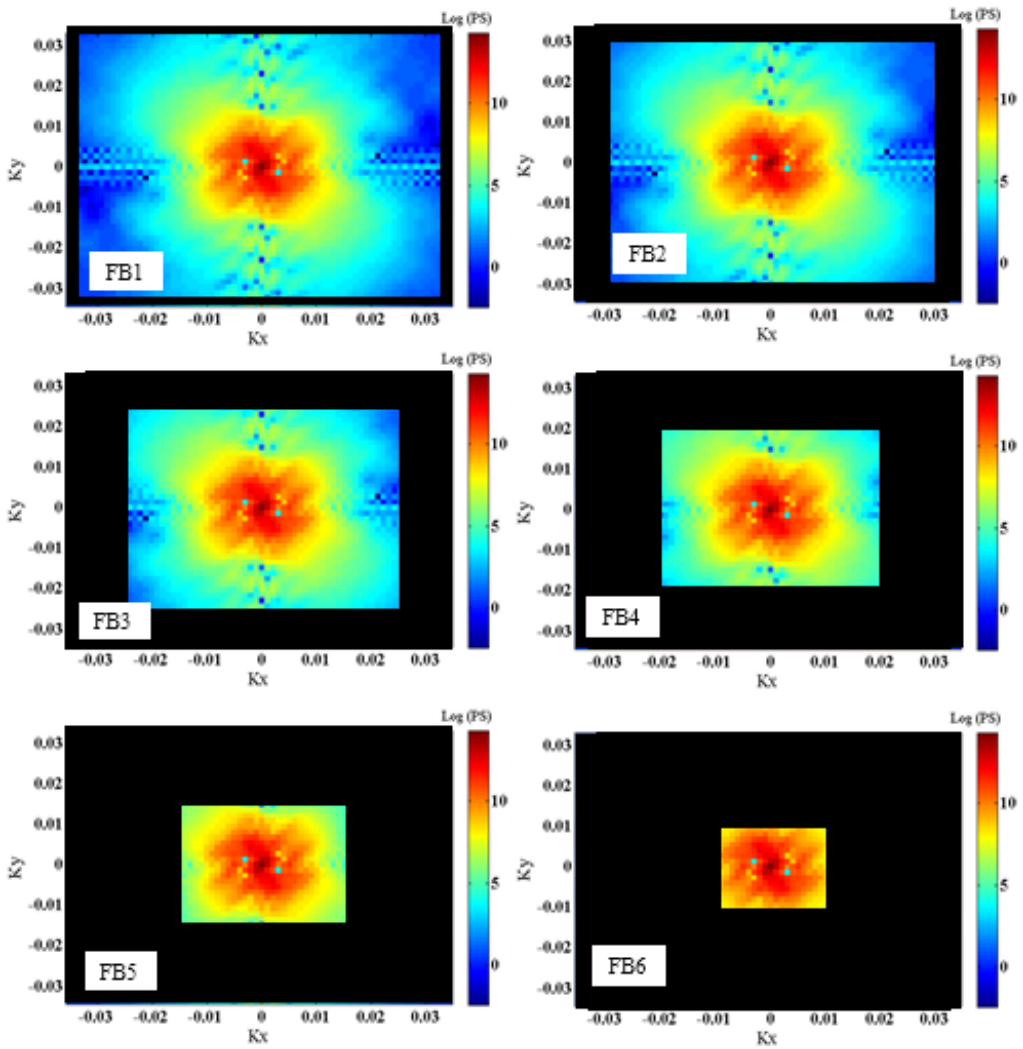

Figure 6. The designed filter functions eliminate different wave number levels in any FBs based on the Table 2.

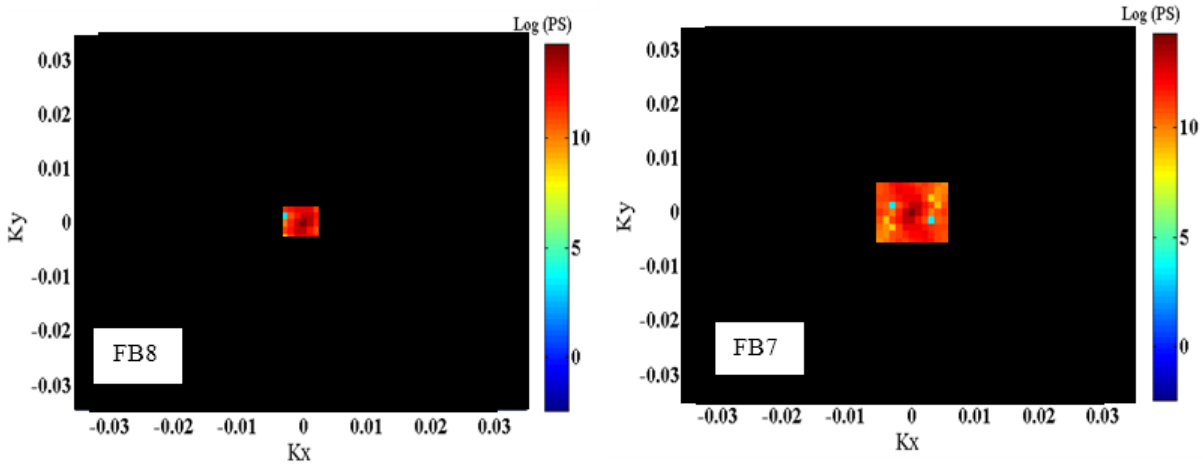

Figure 7. The designed filter functions eliminate different wave number levels in FB7, 8 based on the Table 2.

Table 3. Rotated component matrix for FB2, 7 and 8 using PCA.

	FB2		FB7			FB8		
	Component		Component			Component		
	1	2	1	2	3	1	2	3
Au	0.726	0.577	0.825	0.405	-0.023	0.970	0.174	-0.102
Al	0.956	0.245	0.976	0.136	0.075	0.981	-0.192	0.018
As	0.909	0.338	0.935	0.249	-0.010	0.990	0.007	0.031
Ba	0.065	0.925	0.014	0.937	0.067	-0.074	0.961	0.116
Ca	0.986	0.132	0.992	0.072	-0.007	0.988	-0.096	-0.068
Co	0.595	0.736	0.635	0.715	-0.076	0.951	0.152	-0.257
Cr	0.938	0.262	0.953	0.199	-0.108	0.972	0.010	-0.205
Cu	0.245	0.927	0.228	0.965	0.015	0.233	0.966	-0.088
Fe	0.992	0.087	0.993	0.071	-0.042	0.994	-0.100	-0.040
K	0.959	0.213	0.980	0.077	0.103	0.967	-0.241	-0.033
La	0.991	0.048	0.991	0.037	-0.056	0.991	-0.097	-0.070
Mg	0.852	0.481	0.899	0.374	0.063	0.995	0.052	-0.081
Mn	0.989	0.081	0.992	0.027	-0.017	0.986	-0.144	-0.072
Mo	0.932	0.311	0.956	0.219	0.050	0.989	-0.013	0.076
Na	0.843	0.397	0.890	0.205	0.213	0.920	-0.348	0.018
Ni	0.890	0.380	0.931	0.263	-0.101	0.986	0.041	-0.159
P	0.125	0.940	0.069	0.889	0.133	-0.396	0.832	-0.028
Pb	0.771	0.523	0.850	0.302	0.218	0.958	-0.063	0.254
S	0.098	0.695	0.021	0.141	0.973	-0.076	0.017	0.997
Sc	0.983	0.168	0.993	0.089	-0.002	0.991	-0.124	-0.051
Sr	0.975	0.157	0.981	0.107	-0.020	0.994	-0.060	-0.009
Ti	0.905	0.351	0.941	0.210	0.092	0.996	-0.077	0.028
V	0.971	0.181	0.982	0.093	0.006	0.992	-0.092	-0.063
Zn	0.950	0.245	0.964	0.186	-0.037	0.980	-0.101	-0.037

Table 4. The Variance values of principal components in PCA for FB2, 7 and 8.

Component		Initial Eigenvalues			Extraction Sums of Squared Loadings			Rotation Sums of Squared Loadings		
		Total	% of Variance	Cumulative %	Total	% of Variance	Cumulative %	Total	% of Variance	Cumulative %
FB8	1	19.591	81.631	81.631	19.591	81.631	81.631	19.421	80.922	80.922
	2	2.801	11.670	93.300	2.801	11.670	93.300	2.920	12.168	93.090
	3	1.214	5.057	98.357	1.214	5.057	98.357	1.264	5.267	98.357
FB7	1	18.603	77.511	77.511	18.603	77.511	77.511	17.601	73.338	73.338
	2	2.984	12.434	89.945	2.984	12.434	89.945	3.931	16.378	89.717
	3	1.073	4.470	94.416	1.073	4.470	94.416	1.128	4.699	94.416
FB2	1	18.932	78.885	78.885	18.932	78.885	78.885	16.701	69.588	69.588
	2	3.218	13.410	92.294	3.218	13.410	92.294	5.450	22.707	92.294

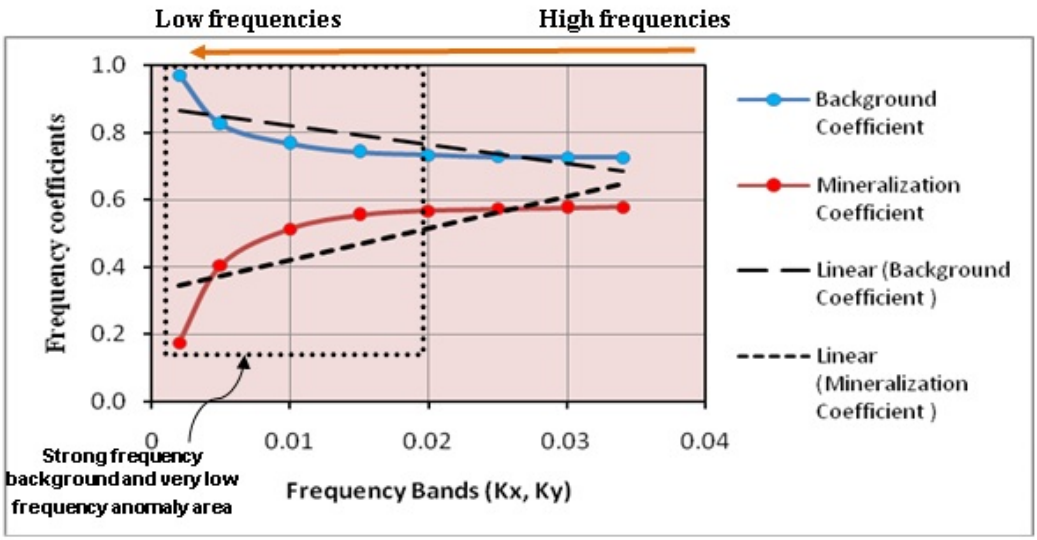

Figure 8. FCM diagram delineated based on the Au frequency coefficients shows a decreasing trend for mineralization from high frequency signals (FB1) to low frequency signals (FB8).

geochemical background and deep mineralization zone are commonly intertwined together in the low FBs. These patterns can be distinguished using the FCM diagram. The mineral deposits with various depths can create the different geochemical anomalies in the spatial domain and the different frequency anomalies in the FD. In deep dispersed mineralized zones, the FCM diagram does not illustrate the strong frequency anomaly in the low FBs. FCM diagram provides the information about the intensity of mineralization at the surface and the depth. Despite the high intensity of surface Au geochemical halo in the studied area (Figure 9), the FCM diagram has predicted that the Au concentration is decreased from the surface to the depth and it is expected to be considered to the non-mineralized zone in the depth. Gold has a more important role in the background component than in the mineralization phase as shown in the FCM diagram (Figure 8). The 6 deep drilled boreholes in the area confirmed these interesting results. The deep boreholes were drilled in this area based on the geochemical, geophysical and geological information (Figure 9). After drilling, several samples were taken from the mineralized cores and analyzed by Atomic Absorption Spectrophotometry at ZGC. These boreholes show very low Au concentrations at depth, suggesting that no mineralized or dispersed mineralization zones are occurring. The results of

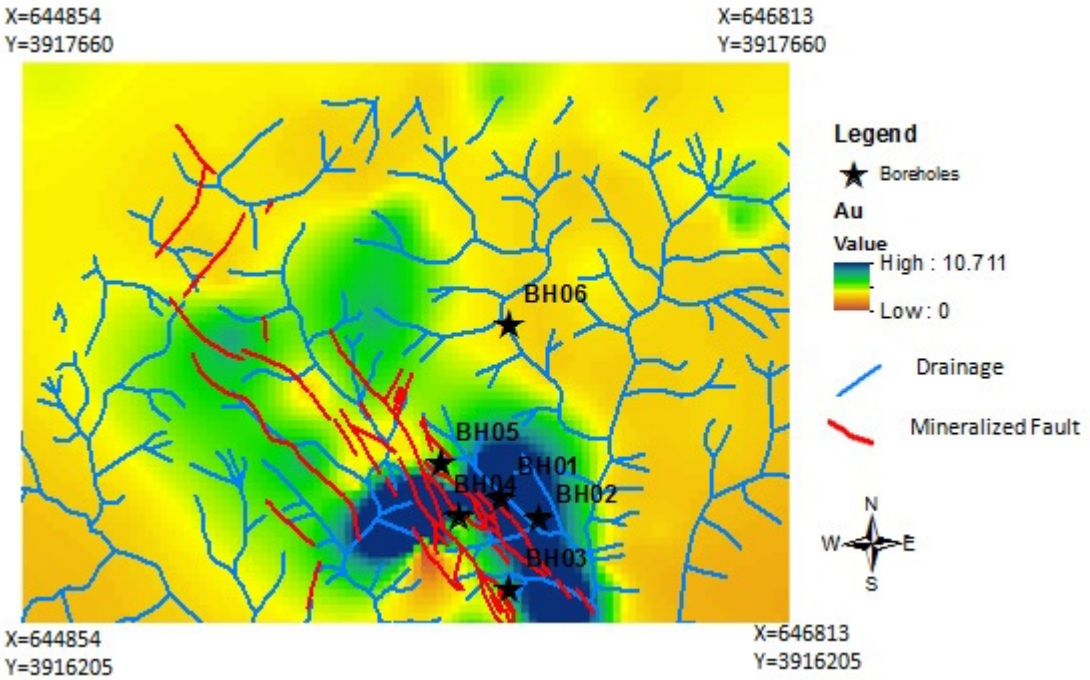

Figure 9. Au geochemical distribution map and locations of deep drilled boreholes in Tanurcheh mineralization area.

boreholes 2 and 6 are summarized in Figure 10.

Three weak mineralization zones are only shown at 100, 230 and 350 m depth in the borehole 2. In this borehole, all mineralized samples had <0.5 mg/kg although most concentrations were <0.2 mg/kg. The deep mineralization in the borehole 6 was weaker than that in borehole 2 and the mineralization zone is poorly seen from the depth of 90 m to 200 m.

FCM can quantitatively present the relationship between the frequency distribution map and the spatial surface geochemical distribution map and allow to depict the intensity of deep mineralization zones at depth. FCM can extract meaningful patterns and exploratory information from the FD of geochemical data.

CONCLUSIONS

In this study, the deep mineralization from the Tanurcheh area (NE Iran) was surveyed by using FCM as a novel approach. FCM, that is defined on the frequency behavior of elements in the mineralization process, was performed on geochemical data from surface samples in FD. The frequency anomalies on the FCM diagram can be related to the important role played by specific elements in the mineralization process and the geochemical anomaly at the specific depths. The obtained results indicated that:

- FCM diagram (Figure 8) displays a decreasing mineralization trend from the high to the low FBs and shows there is no Au frequency anomaly in the FD especially in low FBs. Despite this, the geochemical background has higher values than the mineralization process in the FCM diagram and shows an increasing trend from the high to the low frequency signals. This result shows the low importance of Au mineralization particularly at the depth in this area.

- In spite of the strong Au surface geochemical anomaly and strongly altered rocks at Tanurcheh, FCM predicted there was very weak Au mineralization at depth. This fact was confirmed by the 6 deep boreholes drilled in the area.

FCM can predict and evaluate the situation of the mineralization at the depth without any additional exploratory cost since it is only based on the surface geochemical data.

ACKNOWLEDGEMENTS

I would like to thank to Zarmehr industrial mineral company for providing access to the data base and express special thanks to Mr. Majeed Esmaeelpour for some protection.

REFERENCES

Beus A.A. and Grigorian S.V., 1977. Geochemical Exploration Methods for Mineral Deposits. Applied Publishing Ltd., Wilmette, Illinois. 287 pp.

Cao L. and Cheng Q., 2012. Quantification of anisotropic scale invariance of geochemical anomalies associated with Sn-Cu

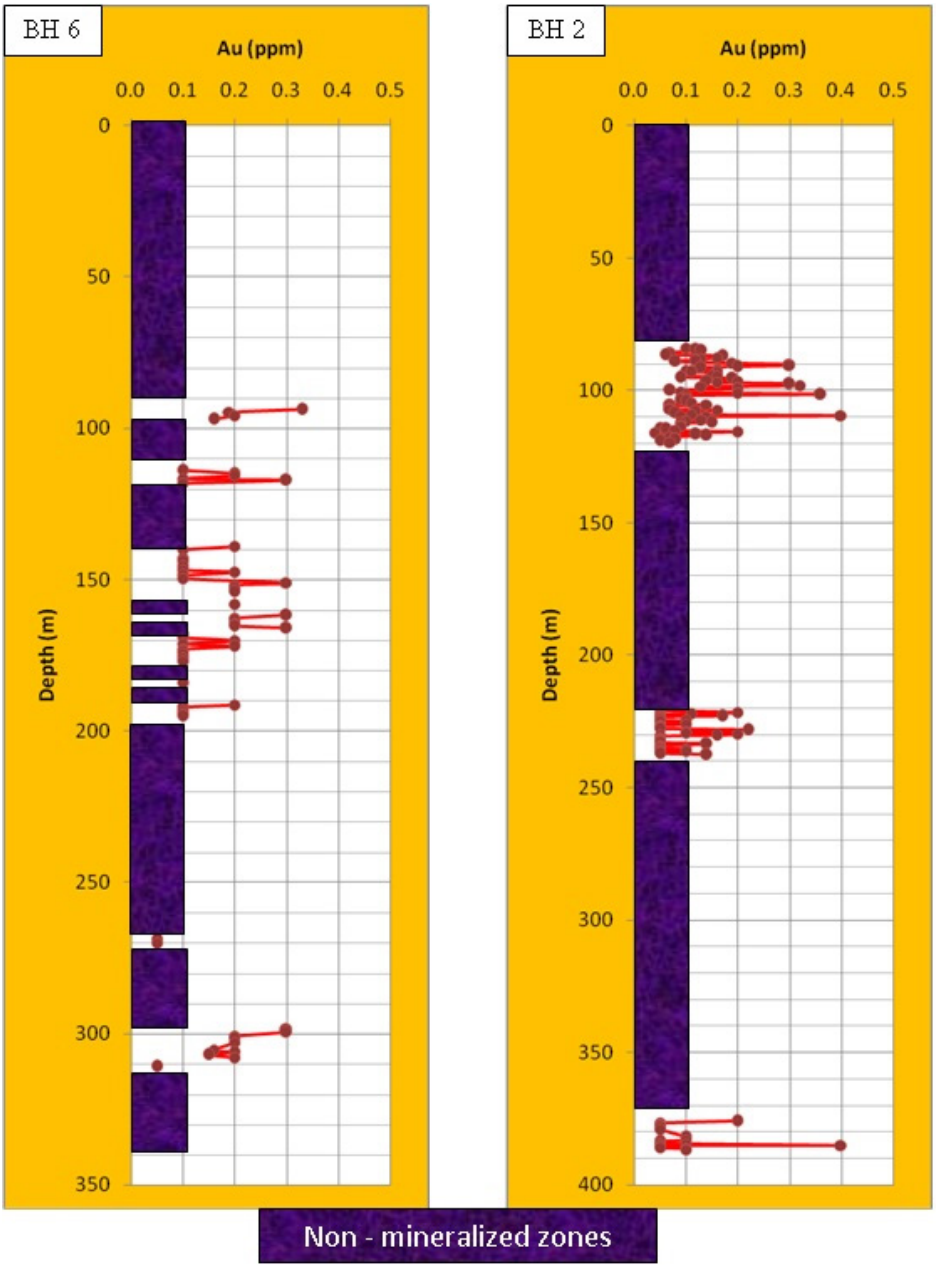

Figure 10. The boreholes 2 and 6 drilled in Tanurcheh Au mineralization area show non-mineralization and dispersed zone at the depth.

mineralization in Gejiu, Yunan Province, China, Geochemical Exploration 122, 47-54.

Carranza E.J.M. and Sadeghi M., 2012. Primary geochemical characteristics of mineral deposits-Implications for exploration. Ore Geology Reviews 45, 1-4.

Cheng Q., 1999. Spatial and scaling modelling for geochemical anomaly separation. Journal of Geochemical Exploration 65, 175-194.

Cheng Q., 2012. Singularity theory and methods for mapping geochemical anomalies caused by buried sources and for predicting undiscovered mineral deposits in covered areas. Journal of Geochemical Exploration, 122, 55-70.

Cheng Q., 2014. Vertical distribution of elements in regolith over mineral deposits and implications for mapping geochemical weak anomalies in covered areas. Geochemistry: Exploration, Environment, Analysis 14, 277-289.

Cheng Q., Xu Y., Grunsky E., 2000. Integrated Spatial and Spectrum Method for Geochemical Anomaly Separation, Natural Resources Research 9, 43-52.

Cheng Q. and Zhao P., 2011. Singularity theories and methods

for characterizing mineralization processes and mapping geo-anomalies for mineral deposit prediction. Geoscience Frontiers 2, 67-79.

Distler V.M., Yudovskaya M.A., Mitrofanov G.L., Prokof'ev V.Y., Lishnevskii E.N., 2004. Geology, composition, and genesis of the Sukhoi Log noble metals deposit, Russia. Ore Geology Reviews 24, 7-44.

Dobrin M.B. and Savit C.H., 1988. Geophysical prospecting: McGraw-Hill Book Co., New York, 867 pp.

Fyzollahhi N., Torshizian H., Afzal P., Jafari M.R., 2018. Determination of lithium prospects using fractal modelling and staged factor analysis in Torud region, NE Iran. Journal of Geochemical Exploration 189, 2-10.

Garrett R.G. and Grunsky E.C., 2001. Weighted sums-knowledge based empirical indices for use in exploration geochemistry. Geochemistry: Exploration Environment Analysis 1, 135-141.

Ghezelbash R., Maghsoudi A., Carranza E.J.M., 2019a. Performance evaluation of RBF-and SVM-based machine learning algorithms for predictive mineral prospectivity modelling: integration of SA multifractal model and mineralization controls. Earth Science Informatics 12,277-293.

Ghezelbash R., Maghsoudi A., Daviran M., 2019b. Combination of multifractal geostatistical interpolation and spectrum-area (S-A) fractal model for Cu-Au geochemical prospects in Feizabad district, NE Iran. Arabian Journal of Geosciences, 12(5), 152.

Grigorian S.V., 1985. Secondary Lithochemical Halos in Prospecting for Hidden Mineralization. Nedra Publishing House, Moscow.

Grigorian S.V., 1992. Mining Geochemistry. Nedra Publishing House, Moscow.

Gundobin G.M., 1984. Peculiarities in the zoning of primary halos. Journal of Geochemical Exploration 21, 193-200.

Hannington M.D., Santaguida F., Kjarsgaard I.M., Cathles L.M., 2003. Regional-scale hydrothermal alteration in the Central Blake River Group, western Abitibi subprovince, Canada: implications for VMS prospectivity. Mineralium Deposita 38, 393-422.

Hassani H., Daya A., Alinia F., 2009. Application of a fractal method relating power spectrum and area for separation of geochemical anomalies from background. Australian Journal of Basic and Applied Sciences 3, 3307-3320.

Karimpour M., 2004. geological report of Tanurcheh mineralization area, Zarmehr Company.

Levinson A.A., 1980. Introduction to Exploration Geochemistry. Applied Publishing Ltd., Wilmette, USA.

Mahdiyanfar H., 2019. Detection of Mo geochemical anomaly in depth using a new scenario based on spectrum-area fractal analysis. Journal of Mining and Environment, 10, 695-704.

Osgood B.G., 2019. Lectures on the Fourier Transform and its Applications (Vol. 33). American Mathematical Soc.

Parsa M., Maghsoudi A., Yousefi M., Carranza E.J.M., 2017. Multifractal interpolation and spectrum-area fractal modeling of stream sediment geochemical data: imply cations for mapping exploration targets. Journal of African Earth Sciences 128, 5-15.

Shahi H., 2017. Prediction of dispersed mineralization zone in depth using frequency domain of surface geochemical data. Journal of Mining and Environment, 8, 433-446.

Shahi H., Ghavami R., Kamkar Rouhani A., Asadi-Haroni H., 2014. Identification of mineralization features and deep geochemical anomalies using a new FT-PCA approach. Journal of Geopersia 4, 101-110.

Shahi H., Ghavami Riabi R., Kamkar Ruhani A., Asadi Haroni H., 2015a. Prediction of mineral deposit model and identification of mineralization trend in depth using frequency domain of surface geochemical data in Dalli Cu-Au porphyry deposit. Journal of Mining and Environment 6, 225-236.

Shahi H., Ghavami R., Kamkar Rouhani A., Asadi-Haroni H., 2015b. Application of Fourier and wavelet approaches for identification of geochemical anomalies, Journal of African Earth Sciences 106, 118-128.

Shahi H., Ghavami R., Rouhani A.K., 2016. Detection of deep and blind mineral deposits using new proposed frequency coefficients method in frequency domain of geochemical data. Journal of Geochemical Exploration 162, 29-39.

Shokouh Saljoughi B., Hezarkhani A., Farahbakhsh E., 2018. A comparative study of fractal models and U-statistic method to identify geochemical anomalies; case study of Avanj porphyry system, Central Iran. Journal of Mining and Environment 9, 209-227.

Wang H. and Zuo R., 2015a. A comparative study of trend surface analysis and spectrum-area multifractal model to identify geochemical anomalies. Journal of Geochemical Exploration, 155, 84-90.

Wang J. and Zuo R., 2015b. A MATLAB-based program for processing geochemical data using fractal/multifractal modeling. Earth Science Informatics 1-11.

Ziaii M., Abedi A., Ziaii M., 2007. Prediction of hidden ore bodies by new integrated computational model in marginal Lut region in east of Iran. In: Milkereit B. (Ed.), Proc. Exploration 07: Fifth Decennial Internat. Conf. Mineral Exploration, Toronto, Canada, 957-961.

Ziaii M., Carranza E.J.M., Ziaei M., 2011. Application of geochemical zonality coefficients in mineral prospectivity mapping. Computers and Geosciences 37, 1935-1945.

Ziaii M., Doulati F., Ziaei M., Soleymani A.A., 2012. Neuro-fuzzy modeling based genetic algorithms for identification of geochemical anomalies in mining geochemistry. Applied Geochemistry 27, 663-676.

Zuo R., 2011a. Identifying geochemical anomalies associated with Cu and Pb-Zn skarn mineralization using principal component analysis and spectrum-area fractal the Gangdese Belt, Tibet (China). Journal of Geochemical Exploration 111, 13-22.

Zuo R., 2011b. Decomposing of mixed pattern of arsenic using fractal model in Gangdese belt, Tibet, China. Applied Geochemistry 26, S271-S273.

Zuo R., Carranza E.J.M., Cheng Q., 2012. Fractal/multifractal modelling of geochemical exploration data. Journal of Geochemical Exploration 122, 1-3.

Zuo R., Xia Q., Zhang D., 2013. A comparison study of the C-A and S-A models with singularity analysis to identify geochemical anomalies in covered areas. Applied Geochemistry 33, 165-172.

Zuo R. and Wang J., 2016. Fractal/multifractal modeling of geochemical data: A review. Journal of Geochemical Exploration 164, 33-41.